Supplemental Data

Semaphorin 3A is an endogenous angiogenesis inhibitor that blocks tumor growth and normalizes the vasculature

Federica Maione, Fabiola Molla, Claudia Meda, Roberto Latini, Lorena Zentilin, Mauro Giacca, Giorgio Seano, Guido Serini, Federico Bussolino, and Enrico Giraudo

Supplemental Methods

Tissue preparation and histology

Tissues were prepared as previously described for frozen and paraffin embedding for RipTag2, HPV/E2 and K14-HPV16 mice (1-3). Non-transgenic and transgenic mice were anesthetized with 2.5% Avertin and euthanized to remove islets and tissue lesions from the three mouse models. The animals were heart perfused with ice-cold PFA 3.75% (wt/vol) (or 10% zinc-buffered formalin) and pancreas, uterine cervices, skin and control tissues/organs were post-fixed in 3.75% paraformaldehyde or 10% zinc-buffered formalin overnight, subjected to graded dehydration through 50%, 70%, 95%, 100% ethanol, and xylene, and finally embedded into paraffin (Paraplast). Alternatively, they were immersed in 30% sucrose/PBS for ~6 h at 4 °C (for pancreas), embedded without fixation in OCT (Tissue Tek), frozen in dry ice and stored at –80 °C. For paraffin sections, the fixed tissues were dehydrated through graded alcohols and xylene, and embedded in paraffin. Five- and ten-μm-thick paraffin sections were serially sectioned using a Leica 2135 microtome, deparaffinized and rehydrated through an alcohol series then stained with hematoxylin and eosin (H&E) at intervals of 100μm for histopathology and immunohistochemistry. For frozen sections, five, ten and 50 μm-thick sections were cut using a Leica CM1900 cryostat. Sections were air-dried,

fixed in zinc fixative (6,05g Tris, 0,35g Ca $(C_2H_3O_2)_2$, 2,5g $Zn(C_2H_3O_2)_2$, 2,5g ZnCl, 3,8 ml HCl 37%) for 10 minutes or, alternatively, in cold acetone, and subjected to H&E staining. The characterization of neoplastic stages based on H&E staining have been previously reported (2, 4) and was done in a blinder fashion on separate occasions by two investigators.

Antibodies

Goat polyclonal anti-SEMA3A (AF1250, R&D), diluted 1:10; purified rat monoclonal anti-Panendothelial Cell antigen (Meca32) (550563, clone Meca32, BD Pharmingen), diluted 1:100; purified rat monoclonal anti-CD31 (Pecam-1) (550274, clone mec13.3, BD Pharmingen), diluted 1:100; hamster monoclonal anti-CD31 (MAB1398z, Chemicon), diluted 1:20; mouse monoclonal anti-CD31 (m0823 clone JC70A, Dako), diluted 1:50; rabbit polyclonal anti-SEMA3F (AB5471p, Chemicon), diluted 1:50; goat polyclonal anti-Sema3E (EB07541, Everest Biotech) diluted 1:200; goat polyclonal anti-Neuropilin-1 (AF566, R&D), diluted 1:100; goat polyclonal anti-Neuropilin-2 (AF567, R&D), diluted 1:100; Rabbit polyclonal anti-Plexin-A1 (AB23391, Abcam), diluted 1:100; rabbit purified polyclonal anti-Plexin-A1 Ab (AB9602, Chemicon), diluted 1:100; rabbit polyclonal anti-Plexin-A2 (sc-25640, clone H70, Santa Cruz), diluted 1:50; rabbit polyclonal anti-Plexin-D1 (sc-67145, clone H-70, Santa Cruz) diluted 1:50; purified rabbit polyclonal anti-c-Myc (a190-105a, Bethyl), diluted 1:100; Rabbit monoclonal anti-cleaved caspase 3 (asp175, clone 5A1, Cell Signaling), diluted 1:100; rabbit polyclonal anti-Ki67 (AB15580, Abcam), diluted 1:100; rabbit anti-NG2 (Chondroitin sulphate proteoglycan polyclonal) (AB5320, Chemicon), diluted 1:100; rabbit polyclonal anti-SMA (AB5694, Abcam), diluted 1:100; rat monoclonal anti-mouse CD140b (PDGF-Rβ) (14-1402, clone APB5, eBioscience), diluted 1:40; goat polyclonal anti mouse PDGF-Rβ (AF1042, R&D), diluted 1:20; rabbit polyclonal anti-Desmin (AB907, Chemicon), diluted 1:20; goat polyclonal anti-Integrinβ1/CD29 (total β1 integrin) (AF2405, R&D), diluted 1:10; diluted 1:10; purified rat polyclonal anti-CD29 (active β1 integrin) (550531, clone 9EG7, BD Pharmingen), diluted 1:10; rat polyclonal anti-mouse CD49E (α5 integrin) (103807, clone 5H10-27, Biolegend)

diluted 1:50; rat monoclonal anti-mouse F4/80 (macrophages) (MCA497G, clone CI:A3-1, AbD Serotec) diluted 1:100; goat polyclonal anti-Neuropilin-1 (sc-7239, clone C-19 Santa Cruz), diluted 1:1000; rabbit polyclonal anti-VEGF (RB-222-P, NeoMarkers, Thermo Fisher Scientific) diluted 1:100.

Immunohistochemical analysis

Frozen sections were used for immunofluorescence staining as previously described (2, 5). Before use, frozen sections were air-dried and acetone-fixed; in some experiments sections were permeabilized in 0,2% Triton-X 100 in TBS pH 7,4. Paraffin sections were deparaffinized and subjected to graded rehydration as previously reported (as described above in "Tissue preparation and histology**"**). Tissue samples were blocked with 1% BSA (Bovine Serum Albumin) and 5% serum (donkey serum) in TBS (blocking solution) or in protein block serum-free (Dako) for 1h at room temperature. Tissues were incubated with primary antibodies (diluted in 0.5X blocking solution or protein block serum-free) for 1 h at room temperature or overnight at 4°C (see above in "Antibodies" for primary antibodies used and their dilutions). After incubation and washing, samples were incubated with secondary antibodies anti Rabbit Alexa Fluor-488 and Alexa Fluor-555; anti Rat Alexa Fluor-488 and Alexa Fluor-647; and anti Goat Alexa Fluor-488 and Alexa Fluor-555 (Molecular Probes) and counterstained with DAPI Nucleic Acid Stain (Invitrogen). Stainings were analyzed by using a Leica TCS SP2 AOBS confocal laser-scanning microscope (Leica Microsystems). The immunohistochemical analysis of Sema3A and CD31 expression in all the specimens of human normal cervix, CIN3 lesion and cervical cancer was carried out on paraffin sections immersed in 10mM citrate buffer pH 6.0, and microwaved for 10 minutes (600 W) and then allowed to cool to room temperature for 30 minutes. The sections were pretreated with 3% of H_2O_2 for 20 minutes to block endogenous peroxidases and then blocked with protein block serum-free (Dako) for 1h at room temperature. Tissues were incubated with primary antibodies (diluted in 0.5X protein blocking serum-free) overnight at 4°C. After incubation and washing, samples were

incubated with a biotinylated secondary Ab (goat anti-mouse IgG and goat anti-rabbit IgG, Dako, ready to use, rabbit anti-goat Jackson Immuno Research diluted 1:200) for 1h at room temperature and antigens were revealed with 3,3-diaminobenzidine (DAB, Sigma-Aldrich) according to the manufacturer's instructions. Sections were counterstained with hematoxylin and visualized with an BX-60 microscope (Olympus) equipped with a color Qicam Fast 1394-digital CCD camera 12 bits (QImaging Corp.). All immune-localization experiments were repeated three times on multiple tissue sections and included negative controls for determination of background staining, which was negligible.

Determination of number of angiogenic islets, tumor burden and histopathological analysis

Angiogenic islets were isolated by collagenase digestion and counted under a dissecting microscope as previously described (3). Angiogenic islets were identified as those that exhibited a reddish patch or patches in a white nodular background (5). The visual scoring scheme was confirmed by histology as described (3). Pancreas and spleen were dissected, and macroscopic tumors (≥ 1 x 1 mm) were excised and measured with a caliper. Tumor volume (in mm^3) was calculated using the formula $V = a \times b^2 \times \pi / 6$ (for approximating the volume of spheroid), where a and b equal the longer and shorter diameter of the tumor, respectively (5). The volumes of all tumors from each mouse were added to give the total tumor burden per animal. In the regression trials there were no age-matched control comparisons for the 16-week Sema3A-treated mice, since control RipTa2 mice did not survive to 16 weeks in the absence of treatment, and thus the comparison was made to 14-week controls and was statistically significant. Comparisons between groups were analyzed by two-tailed, unpaired Mann-Whitney U-test. A p value less than 0.05 was considered significant. Mice were continuously monitored for signs of hypoglycemic shock or drug side effects and were sacrificed if found cachectic or if body weight loss exceeded 15%. Mice were anesthetized and euthanized.

Real-Time RT-PCR analysis

Total RNA was purified from pools of snap-frozen tissues using TriReagent (Sigma-Aldrich) according to manufacturer's instructions and quantified by the RNA 6000 Nano Assay kit in an Agilent 2100 bioanalyzer (Agilent Technologies). Equal amounts (100 ng) of total RNA were reverse-transcribed by High Capacity cDNA Archive Kit (Applied Biosystems). *Sema3*, *Nrp*s, *Plxn*s, *Itg*s and *Gus* mRNAs were quantitatively analyzed by means of TaqMan® Custom Array run on an ABI PRISM 7900HT Fast Real-Time PCR System (Applied Biosystems). The relative quantification method employed was based on the following arithmetical formula $2^{-\Delta\Delta Ct}$ where $\Delta\Delta C_T$ is the normalized signal level in a sample relative to the normalized signal level in the corresponding calibrator sample (6) (normal islet, E_2-treated normal cervix and normal skin). *Gus* gene was the endogenous control detector employed for normalization. Similar results (not shown) have been obtained with *Rpl19* as housekeeping gene. To measure the amount of Sema3A transcript in the normal stages we performed an absolute quantification by means of real-time RT-PCR using increasing concentration (1x 10^{-5} ng, 1x 10^{-4} ng, 1x 10^{-3} ng, 1x 10^{-2} ng, 1x 10^{-1} ng, 1ng) of mouse Sema3A cDNA (TrueClone, Origene, Rockville, MD) and 100 ng of total RNA obtained from normal islet, cervix and skin. The samples were analyzed by using Mm00436469-m1 TaqMan Gene Expression Assay (Applied Biosystems) to detect mouse Sema3A transcript. Absolute quantification (AQ) permits to calculate the unknown quantity of the gene by relating the PCR signal to a standard curve.

Migration assay

40,000 human aortic smooth muscle cells SMCs (Lonza) and 30,000 Human umbilical vein endothelial cells (HUVECs) were seeded on the upper surface of a polycarbonate 8-µm porous Transwell membrane, as previously described (7). SmBM-2 or EBM-2 medium (Lonza) were added in both chambers, whereas guidance cues, i.e. recombinant Sema3A, Sema3E and Sema3F (R&D Systems) or FCS (not shown), were added in the lower chamber only either in the presence or the

absence of SM-216289 inhibitor (5 μM). After 3-6 hours of incubation, cells on the upper side of the filters were then mechanically removed. SMCs and HUVECs of the filter lower side were then fixed in 8% glutaraldehyde for 30 min and stained with 0.1% crystal violet. Values are mean ± SD of four independent experiments. For the dose-response curve migration experiments with both SMCs and HUVECs 50, 100, 200 and 400 ng/ml of recombinant Sema3A were employed.

Proliferation assay

Primary SMCs at passage 3 were seeded in a 96-well plate at initial concentration of 2000-4000 cells/well in SmBM-2 medium containing 10% FCS and growth factors supplements (Clonetics). The cells were treated with two different concentrations (350 and 700 ng/ml) of recombinant human SEMA3A for 48 hr. Fresh medium and recombinant SEMA3A were replaced after 24 hr. In a separate experiment, cells were plated at the density of 2000 cells/ml in 96-well culture plate; the day after, the medium of half of the culture was substituted with medium without serum and growth factors. SEMA3A was employed at a concentration of 700 ng/ml. After 48 hr of incubation at 37 °C, cell proliferation was analyzed by means of a commercial kit based on the bioluminescent measurement of cellular ATP (ViaLight Plus Kit – Cambrex). Islet tumor cells line derived from RIP-Tag2 tumors (βTC3) (8, 9) murine Lewis lung carcinoma (LL/2), human colorectal carcinoma (HCT-116), and MDA-MB-468 human breast cancer cell lines (ATCC) were grown in a 24-well plate at initial concentration of 10,000 cells/well in DMEM (Sigma) medium containing 10% FCS. Tumor cells were incubated with or without 5 μM of SM-216289 inhibitor in serum-free DMEM and, after 48 hr of incubation, were fixed with 8% glutaraldehyde for 30 min, stained with 0.1% crystal violet and solubilized with acetic acid 10%. The proliferation was measured by spectrophotometry (absorbance, 595 nm), using a microplate reader (Perkin-Elmer). The data shown for each treatment is the mean of four replicates ± SD. βTC3 cell lines were kindly provided by Oriol Casanovas (Catalan Institute of Oncology, Barcelona).

Apoptosis assay

Primary human SMCs at passage 3 were seeded in a 4-well chamber slide at the concentration of 4000 cells/well in complete SmBM-2 medium. Cells were treated with two different concentrations (350 and 700 ng/ml) of recombinant human SEMA3A for 48 hr. Fresh medium and recombinant SEMA3A were replaced after 24 hr. As a positive control, cells were treated with 0.5 μM Campthotecin for 24 hr. After total 48 hr of incubation at 37 °C, cells were fixed in 3% paraformaldehyde for 10 min, permeabilized with 1% Triton-X100 for 15 min, and then incubated with the TUNEL reaction mixture containing TdT and TMR-dUTP (Roche) according to the manufacturer instructions.

Western blotting

To assess the Neuropilin1 expression by human aortic SMCs, total lysates of SMCs and HUVECs as control were obtained adding warm Laemmli buffer (SDS 10%, Tris-HCl 0.5 M, pH6.8, glycerol) and sonicating for 20 sec at 400 Hz. To detect Sema3A, AAV8-treated and untreated RipTag2 tumors were microdissected from the excised pancreas, carefully removing the surrounding exocrine tissue, and then snap frozen (3). Proteins were purified from snap-frozen tumors using TriReagent (Sigma-Aldrich) according to manufacturer's instructions. The lysates were separated by SDS-PAGE electrophoresis and transferred to nitrocellulose membrane (Hybond-C Extra, Amersham Biosciences). After blocking with TBS/3% BSA membranes were incubated with primary Ab overnight at 4°C. Neuropilin1 and Sema3A were detected using a goat polyclonal anti-Neuropilin-1 C-19 (sc-7239, Santa Cruz, diluted 1:1000) and a goat anti-Sema3A (R&D AF-1250, diluted 1:500) Abs respectively. After incubation with a secondary peroxidase-conjugated anti-goat (305-035-003, Jackson Immmuno Research, diluted 1:15000) Ab, proteins were detected with ECL (Perkin-Elmer).

ELISA

Proteins were extracted from normal, angiogenic and tumor islets using the ProteoExtract Subcellular Proteome Extraction kit (539790, Merck). Coating was performed using 2µg/ml of protein fraction diluted in PBS and dispensed (100µl/well) into 96 wells polystyrene microtiter plates (Corning Incorporated). The plate included triplicates of each sample and of BSA 2µg/ml as negative control. After incubation at 4°C over night, plates were washed three times with wash buffer (PBS, 0.1% Tween), and blocked with 5% BSA in wash buffer for 1h at 37°C. Primary antibodies, anti-Sema3A, anti-Sema3F, anti-Sema3E, anti-Neuropilin-1, anti Neuropilin-2, anti-Plexin A1, anti-Plexin A2 and anti-Plexin D1 (see above in "Antibodies" for primary antibodies used and their dilutions) were diluted in 5% BSA in wash buffer and added to the plate. After incubation at 37°C for 1h, plate was rinsed three times with wash buffer and the secondary antibodies peroxidase-conjugated was diluted in wash solution and added to the plate (100µl/well). The secondary used antibodies were: Peroxidase-conjugated AffiniPure rabbit anti-goat IgG (305-035-003, Jackson Immuno Research) diluted 1:1000 and Peroxidase-conjugated Fraction Monoclonal Mouse anti-rabbit IgG (221-032-171, Jackson Immuno Research) diluted 1:2500. The plate was incubated at 37°C for 1h and washed again. 1-Step Turbo TMB-Elisa peroxidase substrate (34022, Pierce) was added (100µl/well) and incubated for 5-10 min RT. The reaction was stopped by adding H_2SO_4 2M. The optical density (OD) was measured at a wavelength of 450nm using an ELx800 automated microplate reader (Bio-Tek).

Blood glucose test

A drop of blood (about ten µl) was extracted from the tail vein of non-fasted mice. The blood was then analyzed by a handheld glucose meter (Ascesia Elite; Bayer).

β-gal histochemistry

Tissues were taken from mice and immediately embedded in Tissue OCT (Bio-Optica) for sectioning. 10 μm thick cryostat sections were thaw mounted onto Super Frost Plus microscope slides (Menzel-Glaser) and fixed in 4% paraformaldehyde in phosphate buffer (0.1 M; pH7.6) at room temperature for 5 min. Slides were washed three times in wash buffer (phosphate buffer, 0.1 M pH 7.6, 0.01% sodium deoxycholate, 0.02% Nonidet P-40, 5 mM EGTA, 2 mM MgCl2) and stained in reaction buffer (wash buffer containing 5 mM potassium ferrocyanide, 5 mM potassium ferricyanide, and 1 mg/ml X-gal) overnight at 37°C. The reaction was stopped by immersion in wash buffer followed by counterstaining with Nuclear Fast Red.

References

1. Inoue, M., Hager, J.H., Ferrara, N., Gerber, H.P., and Hanahan, D. 2002. VEGF-A has a critical, nonredundant role in angiogenic switching and pancreatic beta cell carcinogenesis. *Cancer Cell.* **1**:193-202.

2. Giraudo, E., Inoue, M., and Hanahan, D. 2004. An amino-bisphosphonate targets MMP-9-expressing macrophages and angiogenesis to impair cervical carcinogenesis. *J. Clin. Invest*. **114**:623-633.

3. Parangi, S., Dietrich, W., Christofori, G., Lander, E.S., and Hanahan, D. 1995. Tumor suppressor loci on mouse chromosomes 9 and 16 are lost at distinct stages of tumorigenesis in a transgenic model of islet cell carcinoma. *Cancer Res*. **55**:6071-6076.

4. Bergers, G., Javaherian, K., Lo, K.M., Folkman, J., and Hanahan, D. 1999. Effects of angiogenesis inhibitors on multistage carcinogenesis in mice. *Science* **284**:808-812.

5. Bergers, G., Song, S., Meyer-Morse, N., Bergsland, E., and Hanahan, D. 2003. Benefits of targeting both pericytes and endothelial cells in the tumor vasculature with kinase inhibitors. *J. Clin. Invest*. **111**:1287-1295.

6. Vacca, A., et al. 2006. Loss of inhibitory semaphorin 3A (SEMA3A) autocrine loops in bone marrow endothelial cells of patients with multiple myeloma. *Blood* **108**:1661-1667.

7. Serini, G., et al. 2003. Class 3 semaphorins control vascular morphogenesis by inhibiting integrin function. *Nature* **424**:391-397.

8. Efrat, S., et al. 1988. β-cell lines derived from transgenic mice expressing a hybrid insulin gene-oncogene. *Proc. Natl. Acad. Sci. USA* **85**, 9037–9041.

9. Casanovas, O., Hicklin, D.J., Bergers, G., and Hanahan, D. 2005. Drug resistance by evasion of antiangiogenic targeting of VEGF signaling in late-stage pancreatic islet tumors. *Cancer Cell* **8**:299-309.

Supplemental Figure Legends

Supplemental Figure 1. Gene expression profile of *Sema3* and their receptors during K14-HPV16 tumorigenesis. (**A**) In K14-HPV16 mice, Real-Time RT-PCR analysis revealed, compared to N, an up-regulation of *Sema3a* and *Sema3f* mRNAs in Dys that was subsequently down-modulated in SCC. (**B**) *Nrp1* and *Nrp2* transcripts increased in Dys and SCC compared to normal stages. (**C**) *Plxna1, Plxnd1* and *Plxnb1* mRNA expression was up-regulated in both Dys and SCC compared to N. *Plxna2* expression increased in Dys and decreased in SCC. Normalized Relative Quantification (RQ) values are compared to normal stages and are mean ± SD of 4 experiments; Sema3A transcript was present in significant amounts (pg per 100ng of total RNA) in normal skin (Sema3A= 41 pg; see Supplemental Methods). Values were normalized with the endogenous *mGUS* housekeeping gene. RNAs derived from pool of tissue lesions of 10 mice per stage. N= normal skin, Dys = dysplastic skin; SCC= squamous cell carcinoma.

Supplemental Figure 2. Protein expression levels of Sema3 and their receptors during RipTag2 tumorigenesis. Protein levels of Sema3, Nrps and Plxns in RipTag2 mice were measured by ELISA. (**A**) In agreement with Real-Time RT-PCR data, Sema3A, Sema3F and, to a lesser extent, Sema3E proteins were up-regulated in A of RipTag2 mice and down-regulated in T, as compared to N. (**B**) Nrp1 and Nrp2 expression increased in both A and T compared to normal stages (N). (**C**) Compared to N, PlxnA1 and PlxnD1 proteins were up-regulated in both A and T. In contrast, PlxnA2 increased in A and decreased in T. Results are mean ± SD of three replicates. Statistical analysis was performed using Mann-Whitney test.

Supplemental Figure 3. **Cell type-specific localization of Sema3F during RipTag2 and HPV/E_2 tumor progression.** (**A**) Fluorescent confocal microscopy analysis of RipTag2 mice revealed that Sema3F was present in normal epithelial cells (N), highly up-regulated in dysplastic epithelium (A)

(arrows), and inhibited in T, as assessed by Sema3F (red) and Meca32 (green) immunostaining. No Sema3F expression was observed in ECs. (**B**) Sema3F was expressed in basal squamous epithelium of N/E_2 and CIN-3 (arrowheads) and in peri-vascular cells proximal to CIN-3 areas (arrows) as detected by co-localization of Sema3F (red) with Meca32 (green). Sema3F was absent in SCC. Confocal analysis has been performed on tissue sections from 10 mice per stages of both models and images are representative of five fields observed per stages. E, epithelium; S, stroma; T, tumor. Scale bars: 50 μm.

Supplemental Figure 4. **Sema3A and Sema3F expression in stromal cells during HPV/E_2 tumor progression.** (**A**) Fluorescent confocal microscopy analysis of RipTag2 using Sema3A (red) and F4/80 (green) antibodies revealed a subset of Sema3A-F4/80$^+$ cells in the stroma of normal cervix (N/E2) (arrows); an higher number of Sema3A-expressing macrophages was observed in CIN3 lesions (arrows). No Sema3A expression was observed in tumor macrophages. Sema3F (red) was essentially absent from F4/80$^+$ cells (green) in N/E2, CIN3 and SCC. (**B**) Sema3A was not present in PDGF-Rβ$^+$ cells in all the three stages. Sema3F colocalized with PDGF-Rβ$^+$ cells in the stroma nearby to normal epithelium and CIN3 lesions (arrows). Confocal analysis has been performed on tissue sections from 10 mice per stages and images are representative of five fields observed per stages. E, epithelium; S, stroma; T, tumor. Scale bars: 50 μm.

Supplemental Figure 5. Cell type-specific localization of Nrp1, Nrp2, PlxnA1 and PlxnA2 during tumor progression. Fluorescent confocal microscopy analysis of the stages of RipTag2 tumor progression. (**A**) Nrp1 was highly expressed in blood vessels in both A and T compared to N, as detected by co-localization of Meca32 (green) with Nrp1 (red) (arrows). Nrp1 was also present in pericytes (arrowheads and Supplemental Figure 6). Very low Nrp1 expression has been observed in dysplastic epithelium or tumor cells. (**B**) Nrp2 was present in blood vessel in A and T and to a low level in N (arrows), as assessed by Nrp2 (red) and Meca32 (green) immunostaining. Nrp2 was also

present in lymphatic endothelium (arrowheads, data not shown). (**C**) PlxnA1 (red) and Meca32 (green) immunostaining revealed PlxnA1 expression in ECs (arrows) in A and T and, to a lesser extent, in pericytes (arrowheads and Supplemental Figure 6) compared to N. Low PlxnA1 expression was detected in epithelial or tumor cells. **(D**) Compared to N, PlxnA2 was first upregulated in vascular ECs of A stage (arrows) and then disappeared in T, as assessed by co-localization of Meca32 (green) with PlxnA2 (red). PlxnA2 was present, in lesser amounts, in pericytes (arrowheads and Supplemental Figure 6). Dotted lines indicate normal islets and lesions surrounded by the normal exocrine pancreas. Confocal analysis has been performed by using frozen tissues sections from 10 mice per stages and images are representative of five fields observed per stages. Scale bars: 50 μm

Supplemental Figure 6. Expression of Nrp1, Nrp2, PlxnA1 and PlxnA2 in pericytes during tumor progression. (**A**) Nrp1 was highly expressed in pericytes in RipTag2 mice in both A and T compared to N, as detected by co-localization of NG2 (green) with Nrp1 (red) (arrows). Nrp1 was also present in ECs (arrowheads and Supplemental Figure 5). (**B**) Nrp2 was present in pericytes in A and T and to a low level in N (arrows), as assessed by Nrp2 (red) and NG2 (green) immunostaining. (**C**) PlxnA1 (red) and PDGF-Rβ (green) immunostaining revealed PlxnA1 expression in pericytes (arrows) in A and T and, at higher levels, in ECs (arrowheads and Supplemental Figure 5), as compared to N. (**D**), PlxnA2 was up-regulated in pericytes of A stage (arrows) and then disappeared in T compared to N, as assessed by co-localization of PDGF-Rβ (green) with PlxnA2 (red). PlxnA2 was present, in a higher amount, in ECs (arrowheads and Supplemental Figure 5). Dotted lines indicate normal islets and lesions surrounded by the normal exocrine pancreas. Confocal analysis has been performed by using frozen tissues sections from 10 mice per stages and images are representative of five fields observed per stages. Scale bars: 50 μm

Supplemental Figure 7. Sema3A re-expression in RipTag2 tumors employing AAV8.

(**A**) AAV8-Sema3A was delivered to pancreas of twelve week-old tumor-bearing RipTag2 *via* abdominal aorta. Immunohistochemical analysis, using an anti-Myc Ab to detect exogenous Sema3A, revealed 50% delivery efficiency in tumor cells of 16-week old RipTag2 mice. Similar infection efficiency was obtained with AAV8-LacZ (not shown). (**B**) Sema3A was expressed in Riptag2 tumors in its full-length active form (95 kDa) and minimal amounts of degradation products were detected by Western blot analysis of AAV8-Sema3A-infected tumors in comparison to control insulinomas where Sema3A was barely detectable. An anti-Sema3A Ab has been used for the analysis. These images are representative of four different AAV8-Sema3A-treated and untreated RipTag2 mice and the experiments have been repeated three times. Scale bars: 50 μm.

Supplemental Figure 8. Sema3A induces apoptosis in tumor vessels lacking of pericytes in short trials. (**A-C**) Sema3A re-expression in RipTag2 tumors increased pericytes content compared to untreated mice in short regression trials. Mural cells were evaluated by fluorescent confocal microscopy analysis employing antibodies that recognized either NG2, or α-smooth muscle actin (SMA), or PDGFR-β. Bar graphs show the pericytes content by means of fluorescence intensity and a quantification analysis revealed an increased in the pericyte content by 43% for $NG2^+$ cells (**A**), 44% for SMA^+ cells (**B**), and 41% for PDGFR-β^+ cells (**C**) in AAV8-Sema3A-treated vs. untreated tumors (**$p<0.001$). (**D**) The pericyte coverage of tumor blood vessels after 2 weeks of AVV8-Sema3A treatment (short trial, 14 week) is similar to that observed in control RipTag2 mice (14 week), as detected by co-localization of Meca32 (green) with NG2 (red). In contrast increased pericyte coverage was detected after 4 weeks of treatment with Sema3A (long trial, 16 week). Similar results were obtained using anti-αSMA and PDGFR-β Abs (not shown). (**E**) Confocal analysis of 2-week long AAV8-Sema3A treatment revealed that Sema3A induced apoptosis in tumor vessels lacking of pericytes coverage as assessed by PDGFR-β (blue), CD31 (green) and activated caspase-3 (red) co-localization. No significant levels of cleaved caspase-3 have been

observed in tumor endothelial cells covered by mural cells. Arrows show pericyte co-localization with ECs; arrowheads indicate apoptotic tumor ECs lacking of pericytes coverage. Images are representative of five fields per mouse from a total of 10 mice per two and four week-long treatments. Scale bars: 50 μm.

Supplemental Figure 9. Sema3A enhances motility, but does not affect proliferation and apoptosis of smooth muscle cells. Human recombinant Sema3A (50, 100, 200 and 400 ng/ml), enhanced human aortic smooth muscle cells (SMCs) migration (**A**) and inhibited EC motility (**B**) in a dose-response curve as revealed by chemotaxis assays. Relative cell migration is expressed as fold increase compared to control unstimulated cells. SMCs were plated in complete medium in 96-well plate at an initial density of 2000 cells/well (**C**, **E**) or 4000 cells/well (**D**) and Sema3A was added twice every 24 hr. The effects of Sema 3A on SMC cells proliferation was also tested in the absence of serum and growth factors (**E**). No effects on proliferation by Sema3A have been observed in SMCs in all three experimental conditions. (**F**) SMCs were plated in complete medium in 4-well chamber slide and Sema3A was added twice every 24 hr. Treatment with Campthotecin at the concentration of 0.5 μg/ml for 24 hours was used as positive control of apoptosis. TUNEL assay detected no difference in apoptosis in Sema3A-treated *vs.* untreated SMCs. Values for each treatment are mean of four replicates ± SD. (**G**) Western Blot analysis of SMCs lysates employing an anti-Nrp1 Ab revealed a significant Nrp1 expression in SMCs used for the migration, proliferation and apoptosis tests, compared to its expression in HUVECs used as positive control. The image is representative of three experiments.

Supplemental Figure 10. AAV8-Sema3A treatment did not inhibit β1 integrin activation in pericytes. (**A**) Bar graph shows increased percentage of total β1 integrins in pericytes ($NG2^+$ cells) in A e T compared to N (increased by 59% in A and by 61% in T compared to N, ***$p<0.0001$). (**B**) Bar graph shows increased β1 integrin activation in pericytes in A and T compared to N, as

detected by active β1 integrin co-localization with NG2 (increased by 48% e in A, **p<0.001; increased by 73% in T compared to N, ***p<0.0001). Notably β1 integrin activation increased by 49% in $NG2^+$ cells of T compared to $NG2^+$ cells of A (**p<0.001). (**C**) Bar graph shows the percentage of active β1 integrins present in tumor $NG2^+$ cells in AAV8-Sema3A-treated compared to untreated tumors. No differences in active β1 integrin level were detected between the two groups. Total and active β1 integrin co-localization was measured as mean fluorescence intensity ratio between red (total or active β1 integrin) and green (NG2) channels. (**D**) Fluorescent confocal microscopy analysis revealed no differences of active β1 integrin in pericytes of AAV8-Sema3A-treated and control tumors, as detected by co-localization of NG2 (green) with active β1 (red). Arrows and arrowheads respectively indicate the active β1 integrin co-localization with pericytes and endothelial cells, which were measured as mean fluorescence intensity ratio between total or active β1 integrins (red) and NG2 (green). Values are mean ± SD (n=10 per treatment group). Scale bars: 50 μm.

Supplemental Figure 11. SM-216289 does not affect directly tumor cell growth. Effect of SM-216289 on β-islet tumor cell lines (βTC3), murine Lewis lung carcinoma (LL/2), human colorectal carcinoma (HCT-116), and MDA-MB-468 human breast cancer cell lines proliferation**,** as assessed by a proliferation assay. Tumor cell lines were grown in absence or presence of SM-216289 (5 μM). After 48 h of incubation proliferation rate has been detected (see Supplemental Methods). No effect of SM-216289 on proliferation has been observed in all tumor cells lines tested. The data shown is the mean of four replicates ± SD.

Supplemental Figure 1

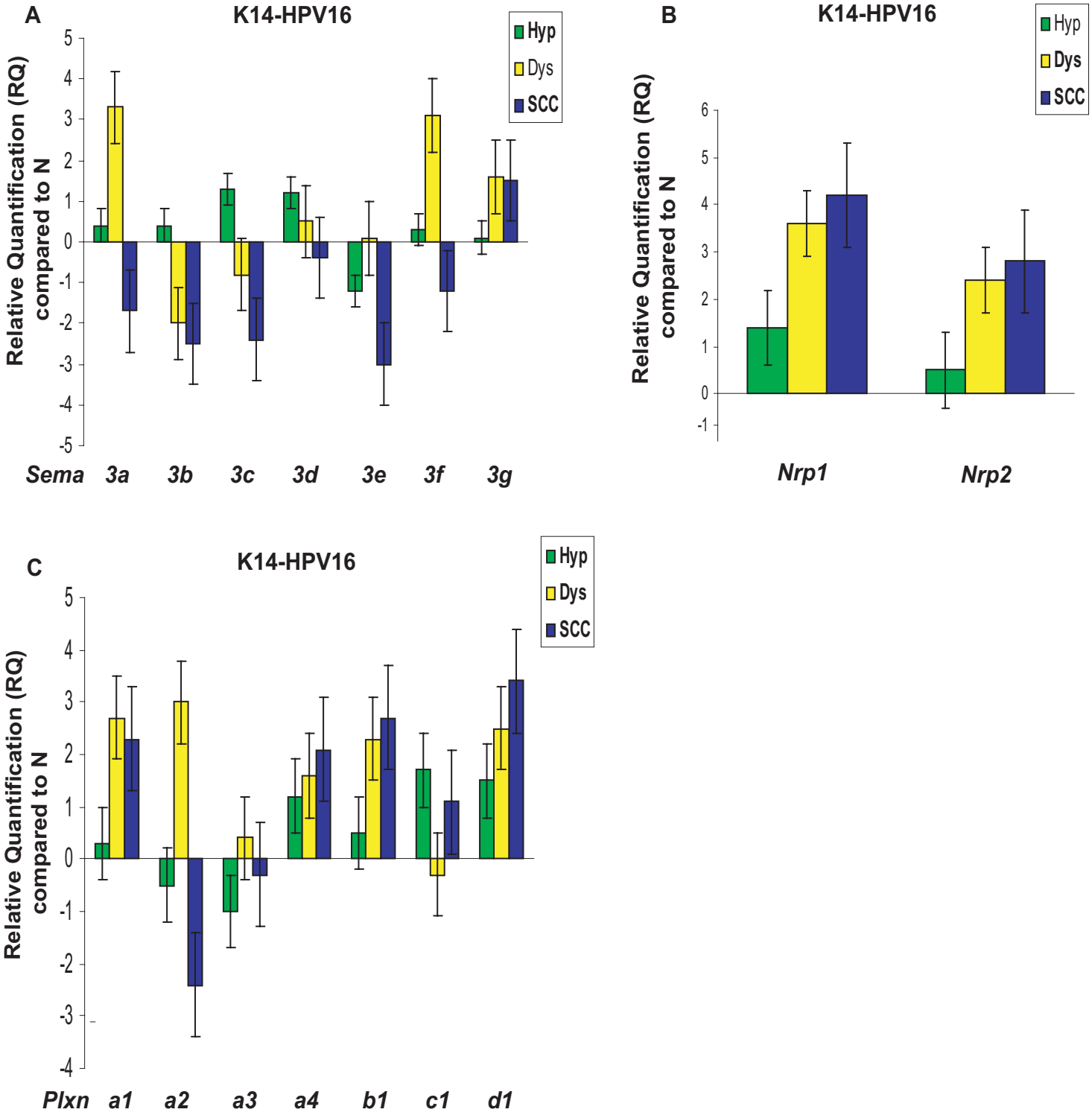

Supplemental Figure 2

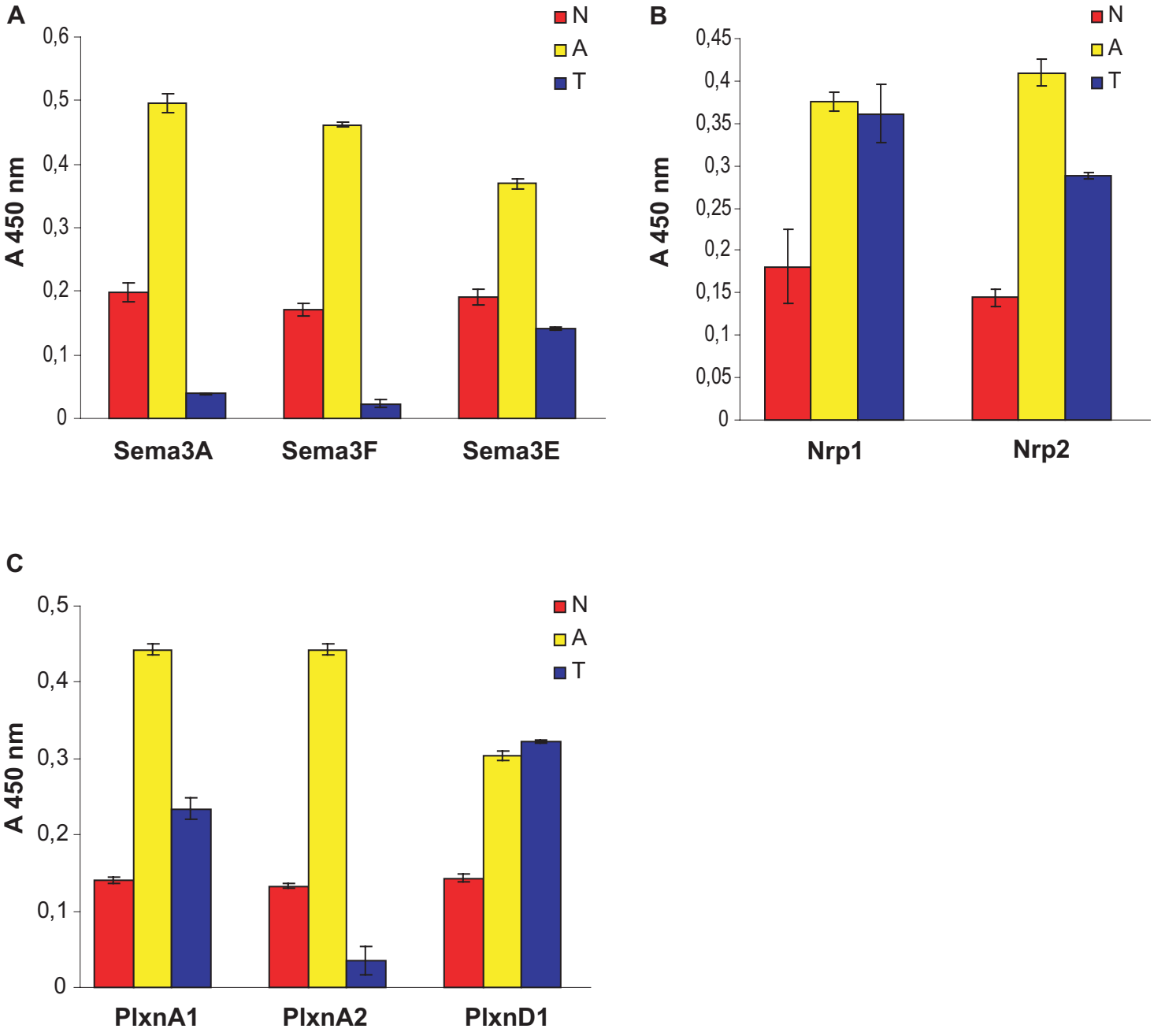

Supplemental Figure 3

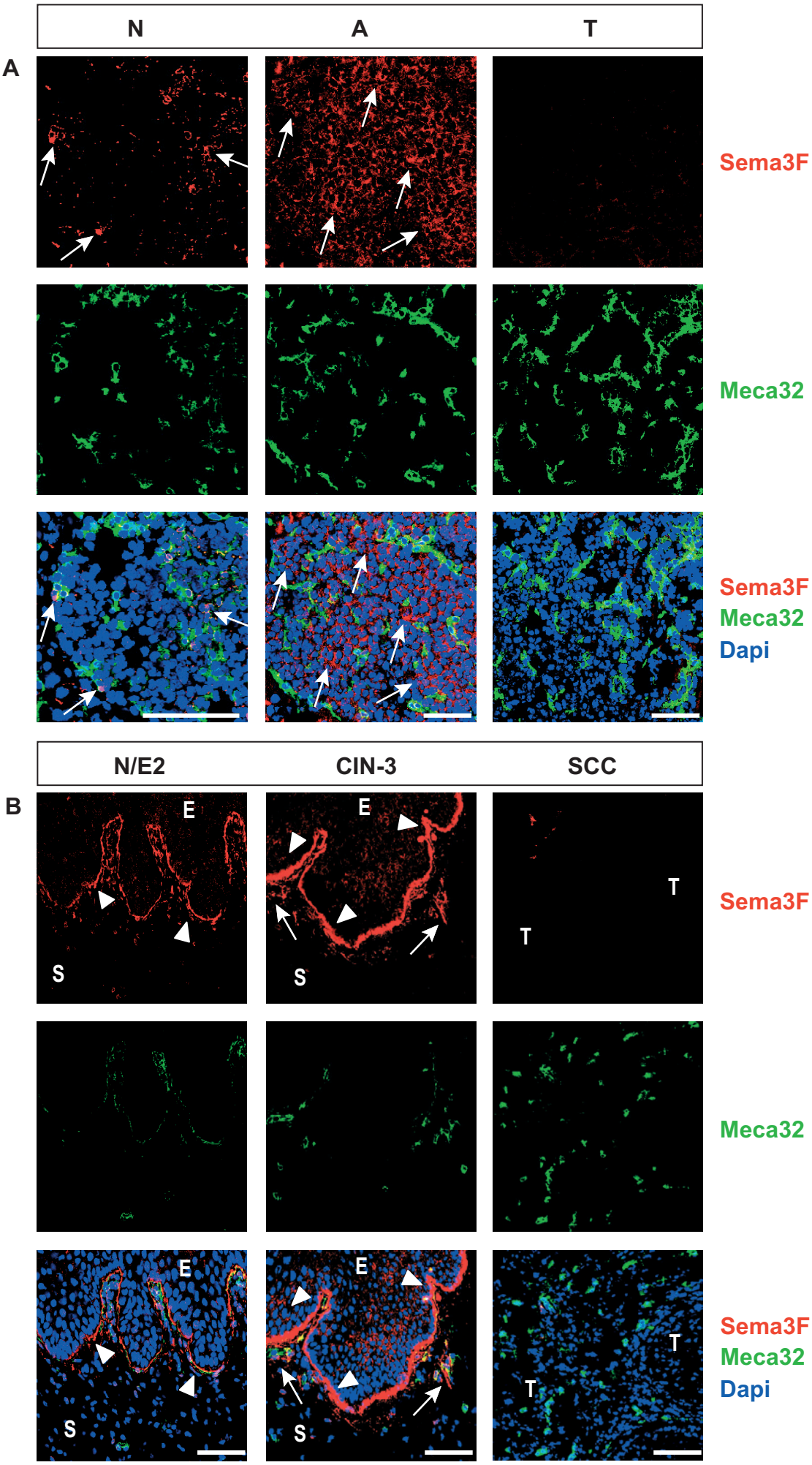

Supplemental Figure 4

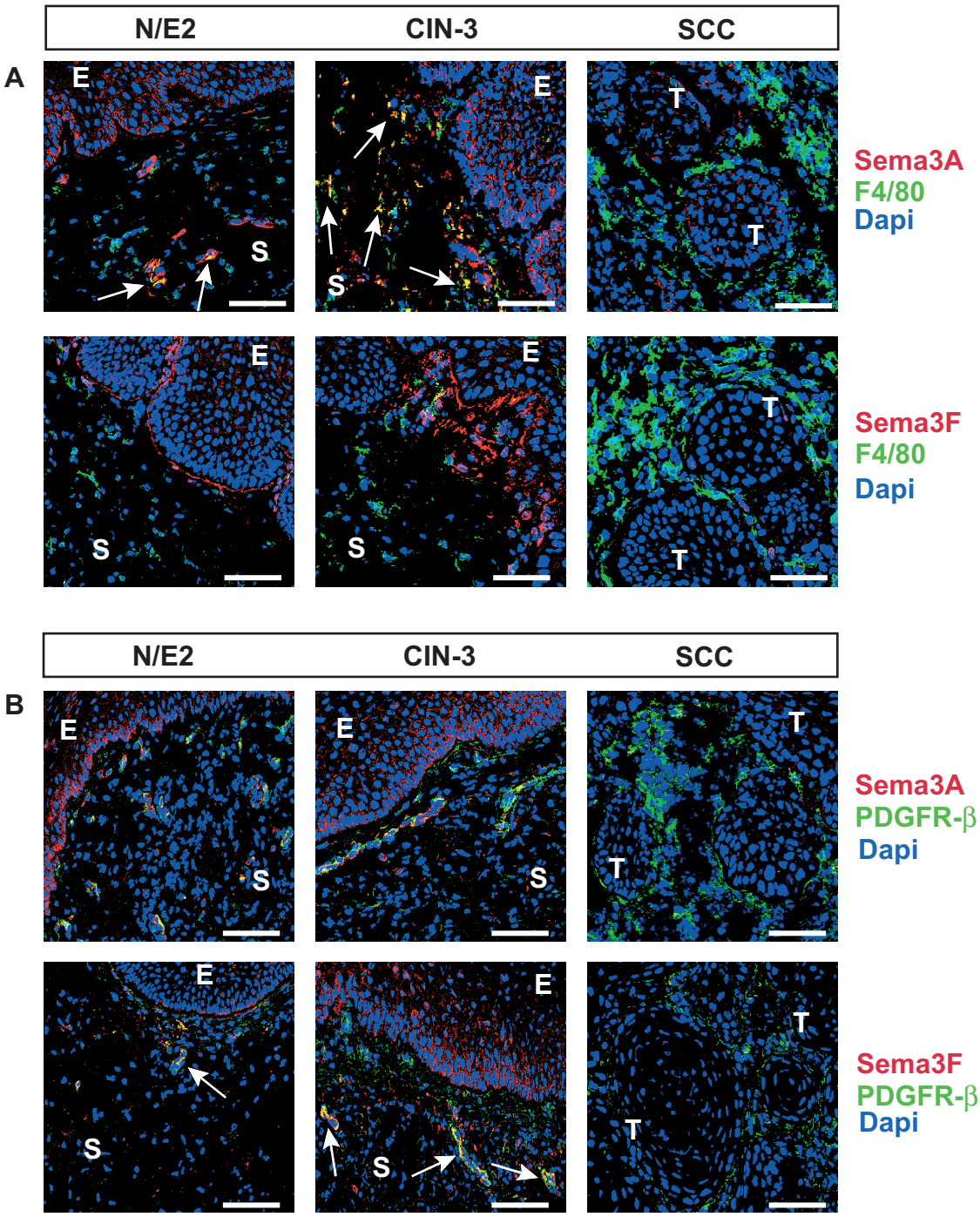

Supplemental Figure 5

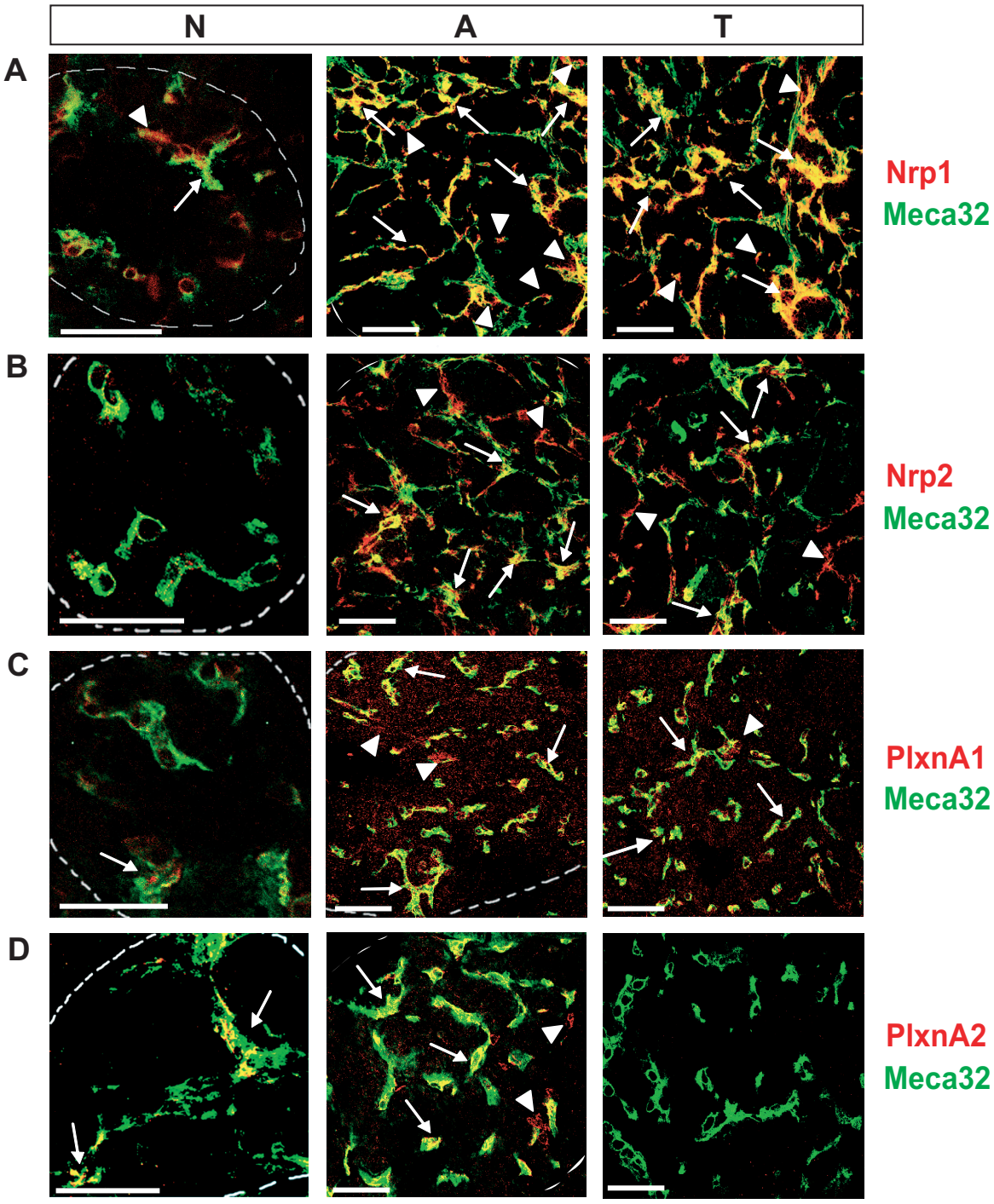

Supplemental Figure 6

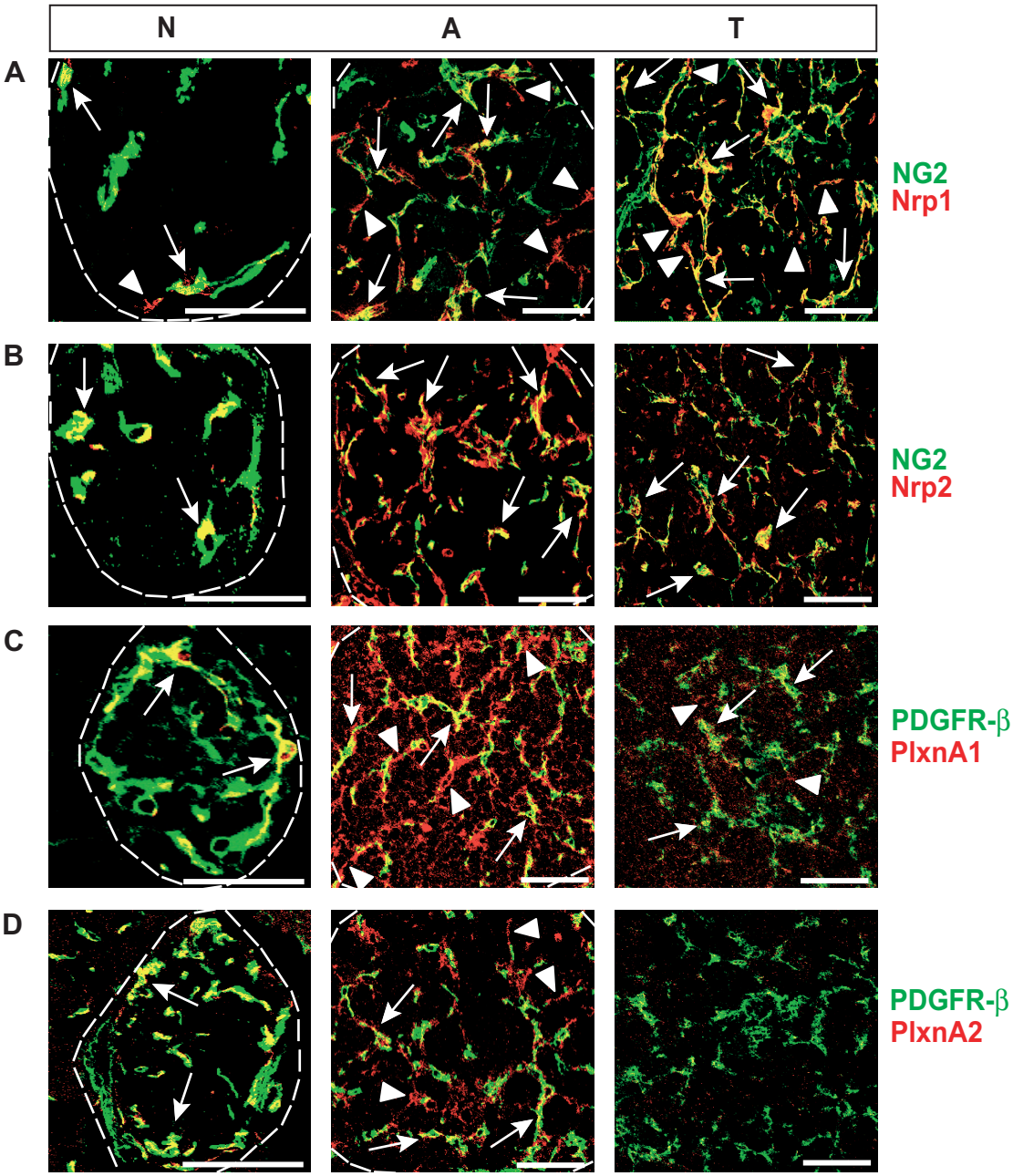

Supplemental Figure 7

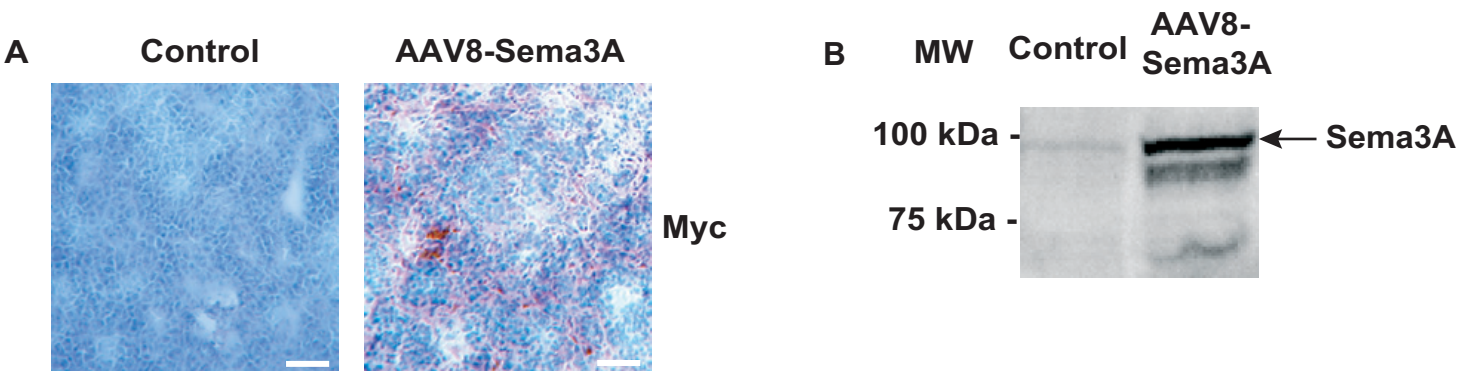

Supplemental Figure 8

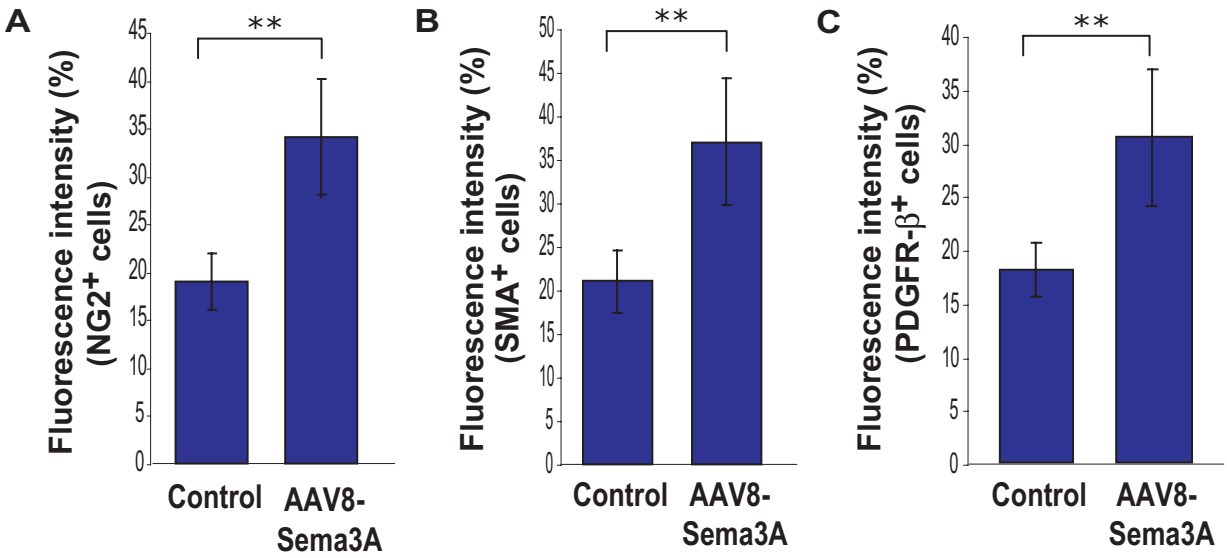

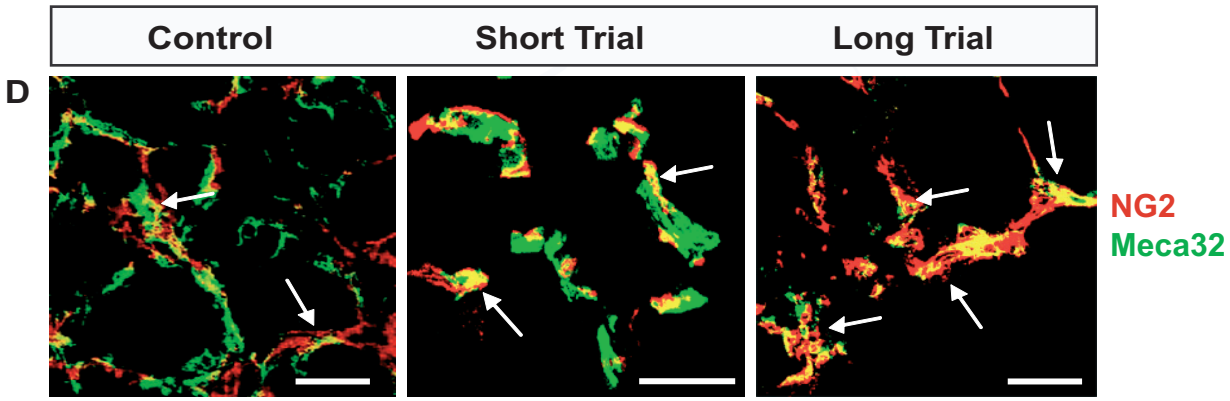

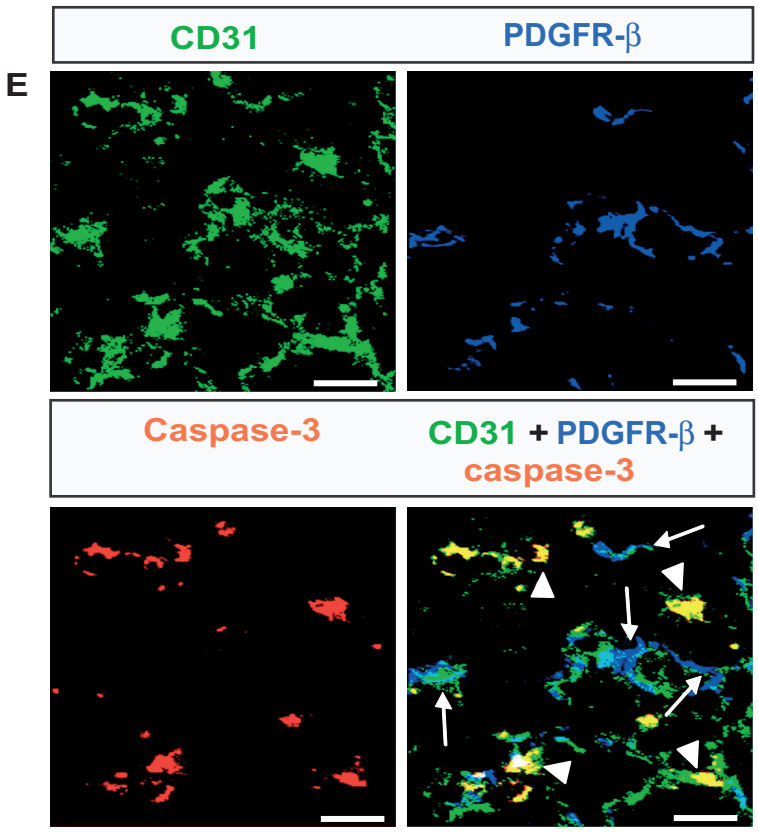

Supplemental Figure 9

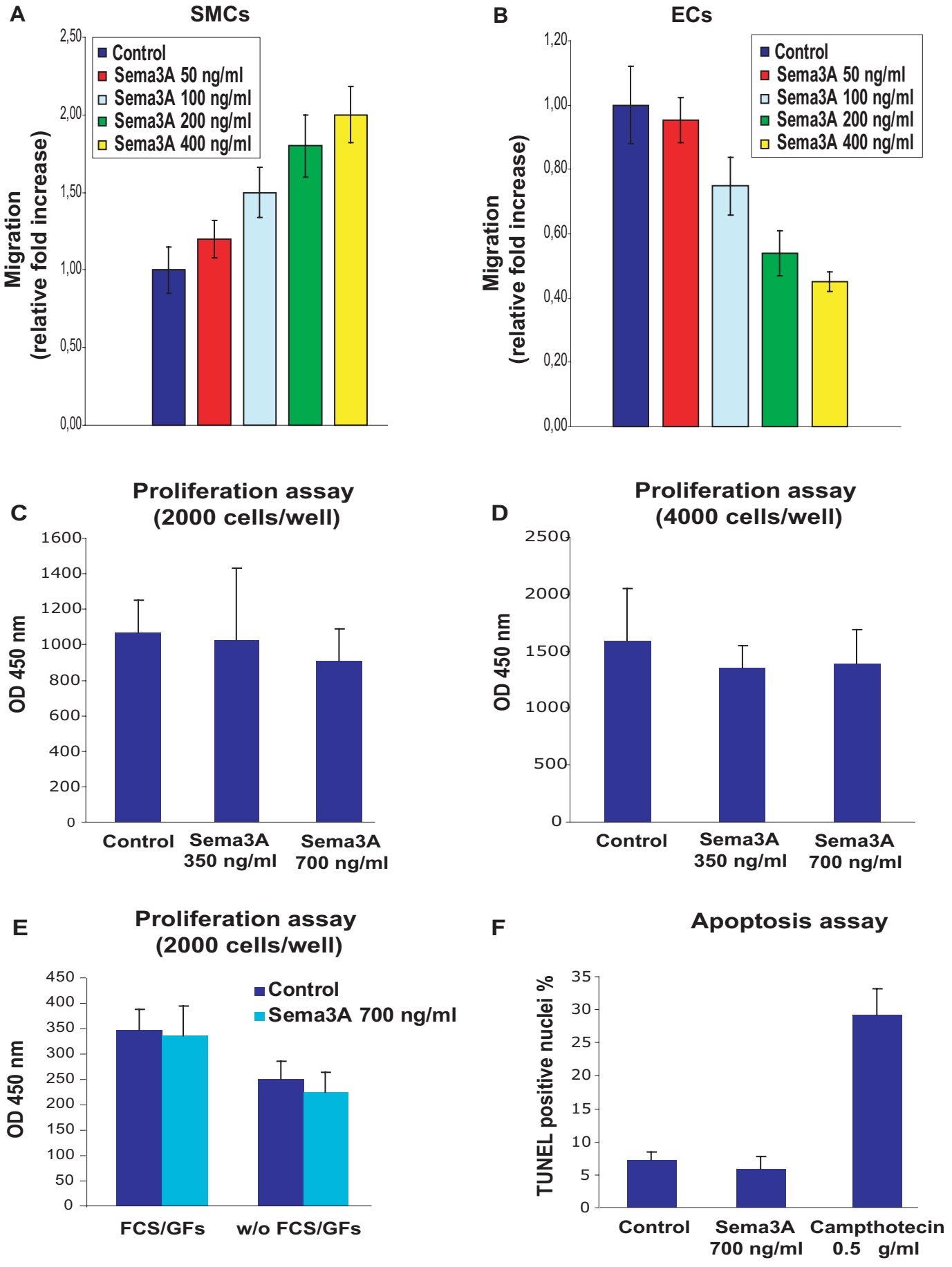

Supplemental Figure 10

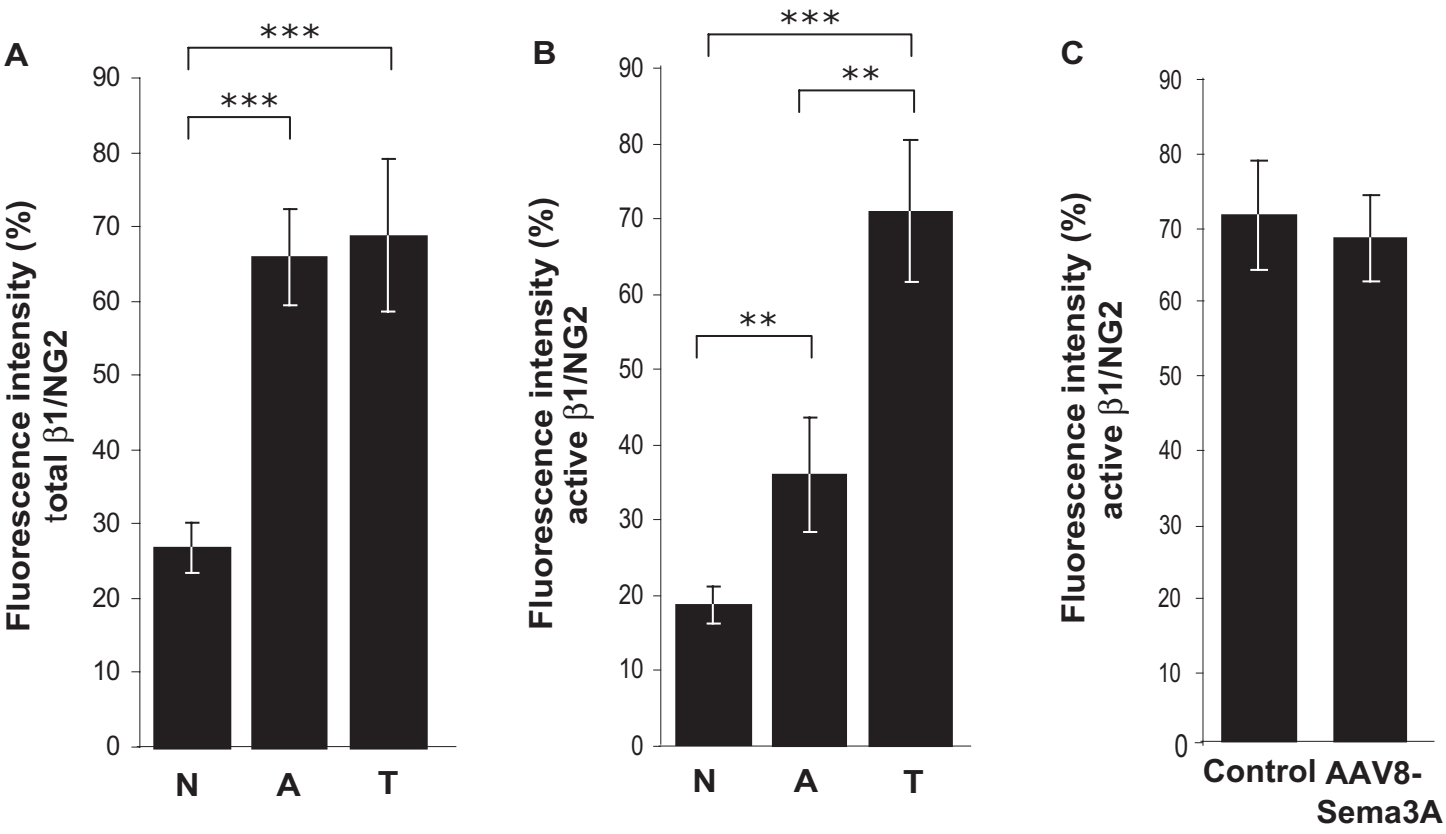

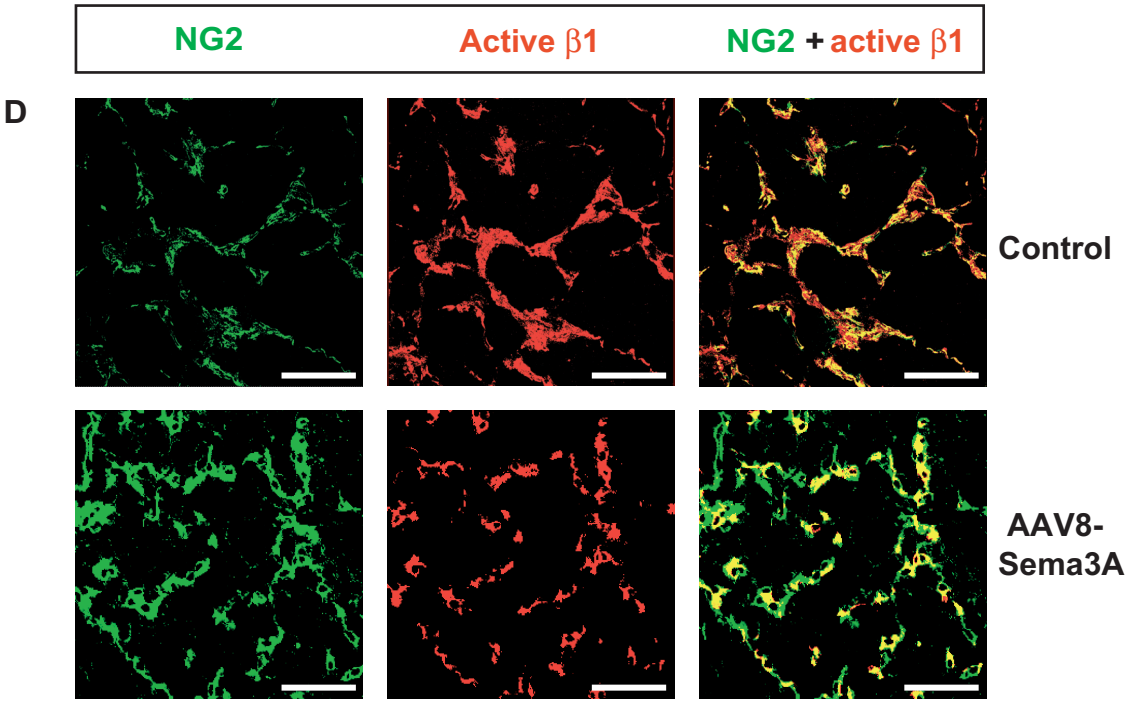

Supplemental Figure 11